

## Weak characteristics of muonium

L. Chatterjee, A. Chakrabarty, G. Das, and S. Mondal

Physics Department, Jadavpur University, Calcutta 32, India

(Received 15 June 1992)

The allowed weak decay channels of muonium are studied in detail. They acquire additional significance in the context of possible  $M$ - $\bar{M}$  oscillations that probe beyond the standard model. The muonium decay rate and annihilation rate are found to be 1.000 023 and  $1.045 \times 10^{-10}$ , respectively, in units of the free muon decay rate.

PACS number(s): 13.35.+s, 12.15.Ji, 36.10.Dr

### I. INTRODUCTION

The muonium atom consisting of a positive muon as the nucleus and an electron is a unique system where an oppositely charged particle-antiparticle pair of different flavors exists in a Coulomb bound state. Composed entirely of nonhadronic constituents, muonium provides an ideal laboratory for fundamental tests of QED and exclusively electroweak interactions. Although the standard model has proved competent in explaining existing experimental findings [1], attempts to dispense with some of its precepts continue. The muonium ( $M$ ) atom acquires additional significance as its possible conversion to antimuonium ( $\bar{M}$ ) provides incisive tests for physics beyond the standard model [2].

The stability of the muonium atom is constantly jeopardized by the strong susceptibility of its muonic nucleus to weak decay. We investigate the different weak decay modes of muonium allowed by the standard model and discuss their relevance to  $M \rightarrow \bar{M}$  experiments [2,3]. Permitting flavor mixing and lepton-number violation, the  $M \rightarrow \bar{M}$  transitions become possible via doubly charged-Higgs-boson or Majorana neutrino exchange [4,5] and this has been experimentally examined [6,2]. The latest report [3] constrains the  $M \rightarrow \bar{M}$  coupling ( $G_{M\bar{M}}$ ) to  $G_{M\bar{M}} < 0.16 G_F$ .

The experimental signatures of the  $M \rightarrow \bar{M}$  are intimately related to the allowed weak decay channels of the muonium, the latter being dominated by the weak decay of its muonic nucleus. The neutrino annihilation exit channel corresponding to weak capture is strongly suppressed because of the nonavailability of the electron at the weak vertex of the muon.

To obtain a comprehensive view of the decay modes of muonium, we have computed the allowed decay modes (Figs. 1–3)

$$(\mu^+ e^-) \rightarrow e^+ + \bar{\nu}_\mu + \nu_e + e^- \quad (\text{via } \mu^+ \text{ decay}), \quad (1)$$

$$(\mu^+ e^-) \rightarrow \bar{\nu}_\mu + \nu_e \quad (\text{via weak capture}). \quad (2)$$

Figure 4 describes the lepton-number-violating  $M \rightarrow \bar{M}$  transition mode.

### II. MUON DECAY FROM MUONIUM

The bare weak decay of the  $\mu^+$  is shown in Fig. 1. Collapsing the intermediate-vector-boson propagator to its local point coupling as justified for such low-energy processes [7], the weak Hamiltonian can be written

$$H_W = (G/\sqrt{2}) [\bar{\psi}_\mu O^\alpha \psi_{\nu_\mu} \bar{\psi}_e O^\alpha \psi_{\nu_e}], \quad (3)$$

with  $O_\alpha = \gamma_\alpha (1 + \gamma_5)$ .

This must be dressed in the Coulomb field of the spectator (Fig. 2). Since the binding is weak and the spatial separation of the spectator is large, the modification of the free rate due to the environment is small and determined by  $a_M$ , the radius of the muonium system.

As the  $M \rightarrow \bar{M}$  precision experiments [2,3] detect the decay lepton and spectator lepton as signals for  $\mu$  decay from  $M$  or  $\bar{M}$ , it seems relevant to reexamine the exact spectrum of these final-state leptons. Interference of slow spectator positrons emitted from the tail of the positron distribution in  $\mu^+$  decay from  $M$ , with the slow positrons expected from  $\bar{M}$  decay and looked for as its signal, could be eliminated by analysis of the distribution. We investigated this process earlier, neglecting mass terms of the recoiling spectator [8]. We dispense with this approximation in the present work and present the spectra of the spectator electron in muon decay from muonium.  $\mu^-$  decay from  $\bar{M}$  would yield the same spectator spectrum for the spectator positron. The matrix element including the bound-state wave function and its overlap with the final spectator can be written as, for bound  $\mu$  decay [4],

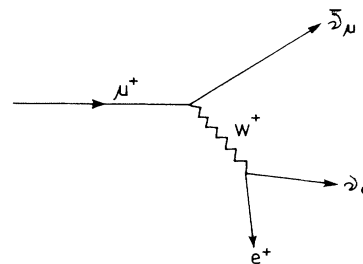


FIG. 1. Bare  $\mu^+$  weak decay.

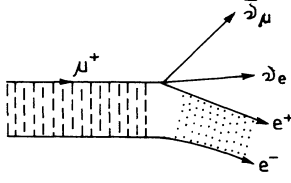


FIG. 2.  $\mu^+$  decay from muonium dressed in Coulomb field of spectator.

$$M_{fi} = H_W I, \quad (4)$$

where

$$I = \int \psi_i(r) e^{i\mathbf{p}_s \cdot \mathbf{r}} d^3\mathbf{r}, \quad (5)$$

$\mathbf{p}_s$  refers to the spectator momentum, and  $\psi_i$  is the initial-state wave function.

The total rate is obtained by integrating the spin-averaged square of  $M_{fi}$  over the final phase space [7]. The neutrinos are integrated over in their center-of-mass frame as for free muon or  $\tau$  decay [7]. Thereafter, shifting to the rest frame of the muonium atom, which is assumed to be coincident with its muonic nucleus, we have

$$\lambda = (CG^2/M_0)[d^3\mathbf{p}_s d^3\mathbf{p}_1 (1/E_s E_1) P_{1\alpha} Q_\beta I_{\alpha\beta} I^2], \quad (6)$$

where

$$I_{\alpha\beta} = (\pi/6)[P_\nu^2 \delta_{\alpha\beta} + 2P_{\nu\alpha} P_{\nu\beta}], \quad (7)$$

$C$  is a relevant constant, and  $\alpha, \beta$  are to be summed over.  $P_1, Q$  are four-vectors of  $e^+$  and  $\mu^+$ , while  $P$  is the total four-momentum carried by the neutrinos.  $E_1, E_s$  and  $\mathbf{p}_1, \mathbf{p}_s$  are the energies and momenta of  $e^+$  and spectator  $e^-$ , respectively.

The kinematic limits on the charged leptonic phase space is obtained from the conservation  $\delta$ -function constraint as

$$2(\sqrt{S} E_1 + p_1 p_s u) + p_1^2 - E_1^2 - 2E_1 E_s = S + E_s^2 - p_s^2 - 2\sqrt{S} E_s, \quad (8)$$

where  $\sqrt{S}$  is the total entrance channel four-momentum given by

$$S = P_0^2 = (P_\mu + P_e)^2 \quad \text{and} \quad u = \cos(\mathbf{p}_1, \mathbf{p}_s). \quad (9)$$

Since the decay lepton is practically a pure Michel one and the distribution heavily favors maximum decay lepton momenta, we take it as massless at present to enable analytic integration of the final phase space.

The maximum value of  $E_1$  is then obtained from Eq. (8) as

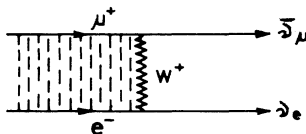


FIG. 3. Muonium annihilation into neutrinos.

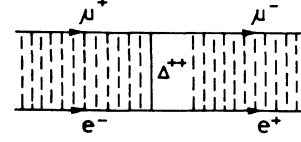


FIG. 4. Muonium going to antimuonium by Higgs-boson exchange.

$$E_1^{\max} = (W^2 - p_s^2) / [2(W + p_s u)], \quad (10)$$

with

$$W = \sqrt{S} - E_s. \quad (11)$$

In contrast, the spectator distribution is strongly peaked at very low momenta and so the spectator mass must be retained. Integrating over the decay lepton and its angle with the final spectator, the spectator spectrum has the form

$$dR_\delta = \frac{32R_f W H^3 K}{a_M^5 m_\mu^4 W_0 M_0 G_0} \frac{x^2}{(x^2 + \eta^2)^4} dx, \quad (12)$$

with

$$G_0 = [(W/W_0)^2 - x^2], \quad x = p_s/W_0 \quad \text{and} \quad \eta = 1/a_M. \quad (13)$$

$W_0$  is the maximum value of  $p_s$ ,  $R_f$  is the free muon decay rate,  $a_M$  is the radius of muonium, and  $M_0$  is the rest mass:

$$H = (S/W_0^2) - x^2 - (2E_s W/W_0^2), \quad (14)$$

$$K = (2W^2/W_0^2) - x^2 - (S/W_0^2) + (2E_s W/W_0^2). \quad (15)$$

The final decay rate is obtained by integrating over the spectator and is reported in Sec. IV.

### III. MUONIUM ANNIHILATION INTO NEUTRONS

It is also important to explore in parallel the muonium annihilation into energy carried by a  $(\nu_e \bar{\nu}_\mu)$  lepton-antilepton pair according to Eq. (2). This was originally discussed by Pontecorvo [9] who obtained  $\sim 10^{-10}$  for its branching ratio to free muon decay from dimensional considerations. We have revisited this process in more detail.

This annihilation process must be completely prohibited from the singlet state of muonium because of helicity constraints (Fig. 5). The final-state  $\bar{\nu}_\mu, \nu_e$  pair must be emitted in opposite directions by momentum conservation as the muonium annihilates practically at rest. As the  $\nu_e$  and  $\bar{\nu}_\mu$  must have opposite helicities, the exit channel selects exclusively the triplet entrance channel. This is similar to the helicity suppression of pion decay by the electronic mode. In the event of the massive neutrino model, however, the process would acquire a finite probability. As the triplet set suffers no such prohibition, muonium annihilation forms a viable mode of muonium disappearance from its triplet state. In dense media the

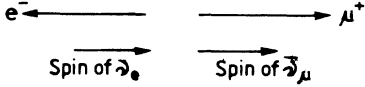


FIG. 5. Suppression of singlet entrance channel for  $M \rightarrow \bar{\nu}_\mu \nu_e$  by helicity constraints.

triplet-to-singlet transition is so fast that the weak capture is not likely to occur. However, in the vacuum scenario, the process could compete with the  $M \rightarrow \bar{M}$  transition if this has a very small coupling constant or its branching ratio is very small. Despite the obvious experimental difficulties involved in detecting an exclusively double neutrino final state, we have computed exactly the process. In case the  $M \rightarrow \bar{M}$  coupling or branching ratio is in reality also negligibly small and the absence of the decay electron of the muon or muonium is noticeable, the interference of the annihilation channel would be important.

The matrix element for  $M \rightarrow \nu_e \bar{\nu}_\mu$  can be obtained from the muon decay case by crossing symmetry by replacing the outgoing positron (Fig. 1) by the incoming electron (Fig. 3).

Energetically, this capture or annihilation mode is favored over pure decay as the electron mass goes into the positive- rather than negative-energy balance. However, it is severely suppressed by the extreme rarity of the electron density  $N_e$  at the weak vertex. As the electron actively participates in the weak dynamics in contrast with its spectating role for channel 1,  $N_e$  acquires crucial importance. The density of electron states  $N_e$  is taken, as for electron capture from atoms by nuclei, as the square of the bound-state wave function taken at contact, i.e.,

$$N_e = |\psi_M(r=0)|^2 = \eta^3 / \pi = 1 / (\pi a_M^3). \quad (16)$$

Since  $a_M \sim (137/m_1)$ , one naively expects a suppression of the rate by of  $\sim 4.45 \times 10^{-14}$  as the relevant factor is  $(a_M/m_\mu)^3$ , when compared with the free muon decay rate. This naive estimate ignores the different phase-space distributions of the final state and any spin dependence of the process. In actual fact the annihilation selects a two-body final state, where the exiting particles are massless or at least effectively so.

In addition, as already mentioned for the singlet-spin state, the reaction is totally forbidden for massless neutrinos, while it is allowed for the triplet state (Fig. 5).

Introducing spin projection operators  $\mathbf{S}_\mu$  and  $\mathbf{S}_e$  for the muon and electron, respectively, and the appropriate phase-space factors for this two-body final state, we have, for the rate,

$$\lambda_a = C_0 \int d^3\mathbf{q}_1 d^3\mathbf{q}_2 \delta^4(P_i - P_1 - P_2) B, \quad (17)$$

where  $C_0$  is the relevant constant and  $B$  is the square of the matrix element summed and averaged over spin states.  $\mathbf{q}_1, \mathbf{q}_2$  and  $P_1, P_2$  refer to the momenta and four-vectors for the two neutrinos.

Using zero-momentum spinors for the muon and electron as is customary for particles in bound states [10] and imposing the identity between the energy and mass components of their four-vectors (i.e.,  $\mathbf{p}_\mu = 0, \mathbf{p}_e = 0$ ), one has

$$B = (P_\mu - m_\mu \mathbf{S}_\mu)(Q_1)(P_e + m_e \mathbf{S}_e)(Q_2) \quad (18)$$

or, on simplifying,

$$B = m_\mu m_e [(E_0^2/4) + (E_0/2)(\mathbf{S}_\mu \cdot \mathbf{q}_1 - \mathbf{S}_e \cdot \mathbf{q}_2) - (\mathbf{S}_\mu \cdot \mathbf{q}_1)(\mathbf{S}_e \cdot \mathbf{q}_2)]. \quad (19)$$

The phase-space integral is trivial for this two-particle final state and yields a constant. Using the momentum  $\delta$ -function dictate  $\mathbf{q}_1 = -\mathbf{q}_2$ ,

$$B = m_\mu m_e [(E_0^2/4) + (E_0/2)(\mathbf{S}_\mu + \mathbf{S}_e) \cdot \mathbf{q}_1 + (\mathbf{S}_\mu \cdot \mathbf{q}_1)(\mathbf{S}_e \cdot \mathbf{q}_1)]. \quad (20)$$

For massless neutrinos,

$$|\mathbf{q}_1|^2 = E_0^2/4 = |\mathbf{q}_2|^2 \quad (21)$$

and

$$B = m_\mu m_e (E_0^2/4) [1 + (\hat{\mathbf{q}}_1 \cdot \mathbf{S}_\mu)(\hat{\mathbf{q}}_1 \cdot \mathbf{S}_e) + (\mathbf{S}_\mu + \mathbf{S}_e) \cdot \hat{\mathbf{q}}_1]. \quad (22)$$

Numerical values are discussed in Sec. IV.

#### IV. RESULTS AND DISCUSSION

The spectator electron distribution for muon decay from muonium is shown in Figs. 6 and 7 for its occupation of different regions of phase space. Figure 6 shows the strong peaking at  $p \sim (\eta/\sqrt{3})$  arising from the overlap of the bound-state wave function with the final spectator. This overlap constrains spectator energy values to within 14 eV for the majority of events and permits the detection of these in the  $M \rightarrow \bar{M}$  probing experiment by acceleration in vacuum. Since the acceleration field accelerates spectating positrons left behind in  $\mu^-$  decay from  $\bar{M}$  to  $\sim 10$  keV energy, the distribution broadens the positron line by about 1.5%. This broadening may not be detectable in the latest experiment as the electric-field inhomogeneity dominates the line and causes an  $\approx 3\%$  correction [3], but may be resolved in future higher-precision experiments. On the other hand, the tail of the

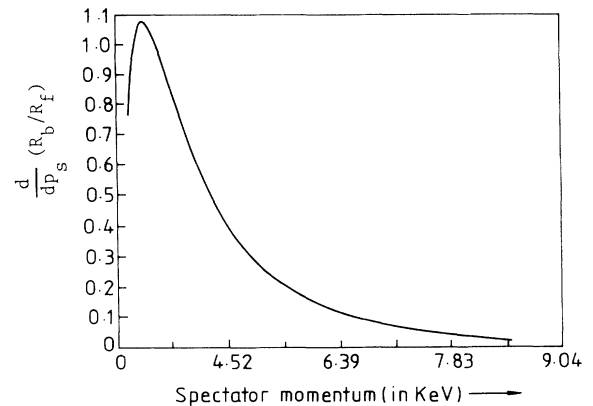


FIG. 6. Differential decay rate in units of free muon decay rate as a function of spectator energy in MeV.

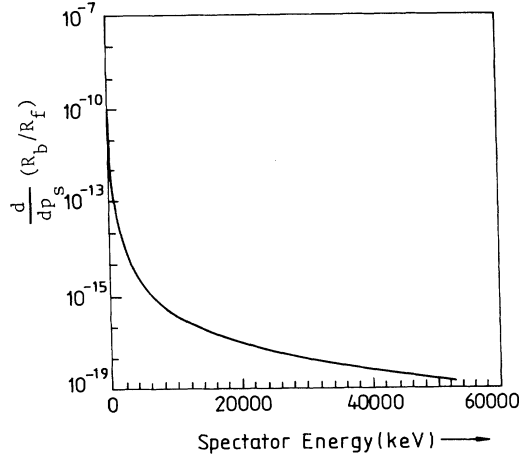


FIG. 7. Suppression of the differential rate for spectator energy in MeV range.

spectator distribution corresponding to its highest values describes the area where the decay is farthest from its Michel maximum and has its lowest energy values. For  $\mu^+$  decay from  $M$ , this corresponds to the emission of very slow positrons which could simulate the positron spectators in the  $M \rightarrow \bar{M}$  conversion event. This region of phase space is, however, suppressed by about 20 orders of magnitude from the peak value, as shown (Fig. 7), and therefore is not expected to cause appreciable violation of the  $M \rightarrow \bar{M}$  detection. Equation (12) can be integrated analytically to yield

$$R = R_b/R_f = (W^5/m_\mu^5)(1 + \{\eta/[\pi W_0(1 + \eta^2/W_0^2)] - \eta^2/W^2\}). \quad (23)$$

Terms of order  $(\eta/W_0)$  and  $(\eta/W_0)^2$  have been retained as higher powers are reduced  $\sim 10^{-12}$  compared with the leading terms.

The term  $(\eta/W_0)$  in Eq. (23) causes the rate to be enhanced slightly over the free muon decay rate as the negative term is smaller and the resultant rate for muon decay from muonium is obtained as 1.000 023 times the

free muon decay rate from Eq. (23).

It should be noted that in the present analyses mass terms of the decay lepton have been neglected as for the normalizing free rate. These would add correction terms of order  $(m_e/m_\mu)^2$  and for massive neutrinos  $(m_{\nu_e}/m_\mu)^2$  and  $(m_{\nu_\mu}/m_\mu)^2$  as usual for both the free decay and decay from muonium. The radiative corrections also would be the same as those for the free decay except for the additional diagrams connecting the muon and decay positron to the spectator. These can be considered equivalent to the continuous exchange of Coulomb photons, giving rise to the bound state in the entrance channel and the Coulomb correction in the exit channel.

The former is accounted for by the bound-state wave functions. Since the spectrum is dominated by the high value of the relative velocity  $v$ , the final-state Coulomb cross section determined by  $\xi = Ze^2/v$  is negligible for this system.

For the muonium annihilation channel, referring to equations (14), for the singlet state,

$$S_\mu = -S_e$$

and

$$B \rightarrow 0$$

by helicity constraints. For the triplet state,

$$B = m_\mu m_e E_0^2.$$

The branching ratio is

$$R_a = \lambda_a/\lambda_f = 1.045 \times 10^{-10},$$

where  $\lambda_a$  is the annihilation rate and  $\lambda_f$  the free  $\mu^+$  decay rate.

#### ACKNOWLEDGMENTS

L. C. would like to thank K. Jungmann, H. K. Walter, and G. M. Marshall for discussions on different sectors of the work. Financial support from the University grant commission and Department of atomic energy is gratefully acknowledged.

- [1] F. Scheck, presented at the Workshop on the Future of Muon Physics, Heidelberg, Germany, 1991 (unpublished).
- [2] H. K. Walter, presented at the Workshop on the Future of Muon Physics [1]. Also PSI experiment proposal. R89-06.1.osal.R89-06.1.
- [3] B. M. Matthias *et al.*, Phys. Rev. Lett. **66**, 2716 (1991).
- [4] A. Halprin, Phys. Rev. Lett. **48**, 1313 (1982). R. N. Mohapatra, in *Proceedings of the 8th Workshop on Grand Unification*, Syracuse, New York, 1987, edited by K. Wali (World Scientific, Singapore, 1987).
- [5] G. Feinberg and S. Weinberg, Phys. Rev. **123**, 1439 (1961).

- [6] G. A. Beer *et al.*, Phys. Rev. Lett. **57**, 671 (1986); G. M. Marshall *et al.*, Phys. Rev. D **25**, 1174 (1982).
- [7] L. Chatterjee and V. P. Gautam, Phys. Rev. D **41**, 1698 (1990).
- [8] L. Chatterjee, S. Bhattacharya, and T. Roy, Acta Phys. Pol. B **11**, 635 (1980).
- [9] B. Pontecorvo, Zh. Eksp. Teor. Fiz. **33**, 549 (1958) [Sov. Phys. JETP **6**, 429 (1958)].
- [10] A. I. Akhiezer and V. B. Berestetskii, *Quantum Electrodynamics* (Interscience, New York, 1965).